Improvement of Agilent 3458A Performances in Wideband Complex Transfer Function Measurement

Improvement of Agilent 3458A Performances in Wideband Complex Transfer Function Measurement

Gabriella Crotti, Domenico Giordano, Mario Luiso, *Member, IEEE*, and Paolo Pescetto

***Abstract*— Digital multimeters (DMMs) Agilent 3458A are valuable devices in accurate characterization of voltage transducers. Five selectable ranges, from 100 mV to 1 kV, high input impedance and accuracy make this device the state of the art. The paper focuses on the correction of the multimeter frequency response when used in Direct Current digitising mode (DCV), to allow post-correction of the errors introduced by the digitizers. To this end, two different approaches for the identification of the multimeter input complex filter function up to about 100 kHz are proposed. They are, respectively, based on the identification of the complex filter transfer function considering the input stage of the DMM as a black box and on the estimation of the parameter of the DMM input stage. The two methods are validated in a test case and equivalence of the results obtained is found. As a further verification, a deep investigation of DCV and direct sampling mode is performed when the zero level trigger mode is set.**

***Index Terms*— Calibration, measurement, power quality, power system measurement, transducer, voltage measurement.**

I. Introduction

WITH the widespread diffusion of renewable energy sources and switching power electronics, the spectral content of the electrical signals in the transmission and distribution grids is becoming rich of tones other than the fundamental component. Therefore the used transducers are required to accurately scale the grid voltage and currents to level compatible with the input of the measuring instruments in a wider and wider frequency range. New sensors with extended performances have been then developed, which entail new and specific calibration setups, with improved features, to verify their accuracy in a frequency range up to the 50th harmonic and over [1], [2]. Moreover, techniques, based on the measurement of synchronized phasors of electrical quantities, are diffusing as new means to gain robust control over dynamically reconfigurable power systems [3]. Thus, new reference setups, which handle with nonsinusoidal signals and time-varying disturbances, are needed.

As to the calibration setups for both conventional and nonconventional voltage sensors and for current sensors with voltage output signal, the requirements for the measuring bridge are, essentially, a wide frequency range, from direct current (dc) up to some tens of kilohertz, and the possibility of comparing signals with very different magnitudes (f.i. 100 mV and 100 V).

In this context, the adoption, as a reference digitizing system, of widespread digital multimeters such as the Agilent 3458A (now Keysight) [4], which are often available in calibration laboratories, can give a strong impulse to the realization of performing and economically efficient reference setups.

Thanks to the high metrological performances, available ranges (from 100 mV to 1 kV) and high input impedance, the use of a synchronized couple of digitizers Agilent 3458A can allow the accurate measurement of the ratio and phase errors of voltage and current transducers for electrical distribution and transmission grids over a wide frequency range. The DCV mode is the most accurate sampling mode (from a few to 100 μV/V) with the highest input impedance. However, with the increase of the frequency, the cutoff frequency of the input low-pass filter, which depends on the selected range [4], becomes the most significant source of errors, in particular when a set of two multimeters working with different ranges are employed in the measurement of the ratio and phase error of a transducer by comparison with a reference one. An accurate characterization of digital multimeter (DMM) performance, including the identification of the actual complex transfer function of the low-pass filter, for each range, can overcome this drawback allowing post-correction of the errors introduced by the digitizers.

Several papers [5]–[13] are focused on the characterization of the Agilent 3458A with the aim to use it as a reference sampling system for alternating current (ac) and dc electrical quantities (ac/dc transfer standard, ratio standard, power standard, etc.).

Some authors [5], [6] propose compensation for voltage dependence of gain and others [7] propose a configuration composed by two synchronized DMMs for accurate measurement of phase at a frequency of about 16 Hz. In [8], a method to correct the phase error due to the digitizing process at low

Manuscript received January 3, 2017; accepted January 10, 2017. This research is funded by the European Metrology Research Program (EMRP), which is jointly funded by the EMRP participating countries within EURAMET and the European Union. The Associate Editor coordinating the review process was Dr. Branislav Djokic.

G. Crotti and D. Giordano are with the Istituto Nazionale di Ricerca Metrologica, 10135 Turin, Italy (e-mail: g.crotti@inrim.it; d.giordano@inrim.it).

M. Luiso is with the Department of Industrial and Information Engineering, University of Campania "Luigi Vanvitelli," 81031 Aversa, Italy (e-mail: mario.luiso@unina2.it).

P. Pescetto is with the Dipartimento Energia del Politecnico di Torino, 10129 Turin, Italy (e-mail: paolo.pescetto@polito.it).

Color versions of one or more of the figures in this paper are available online at http://ieeexplore.ieee.org.

Digital Object Identifier 10.1109/TIM.2017.2661658

frequency, where the effects of the limitation of the bandwidth are quite negligible, is proposed.

Correction methods for the systematic errors introduced by the low-pass input filters are successfully proposed in [9]–[11], respectively, considering a frequency range up to 1 kHz, 3300 Hz, and 400 Hz.

The digitiser frequency response is modeled in [9] by a low-pass one-pole filter with rated cutoff frequency 120 kHz (1 and 10 V range) and 36 kHz (100 V and 1 kV range). Because of the additional error due to input amplifier, a one zero ($f_z = 82$ kHz) and one pole ($f_p = 120$ kHz) low-pass filter is considered for the 100 mV range. By this approach, errors lower than 10 μV/V are obtained at 78 Hz. In [10], 20 μV/V residual errors from 50 to 3300 Hz after finite-impulse response filter equalization are found considering the rated cutoff frequency and an approximated filter description in the case of 1 V digitizer range. A second-order low-pass filter is introduced in [11], which is based on the nominal values of the input circuitry parameters, leading to an agreement between the digitiser optimised response and the ac–dc transfer given by thermal converters better than 2 μV/V for frequencies between 20 and 400 Hz for the 1 V range. Correction methods for a wider frequency range (up to 20 kHz) and for the 10 V range are applied in [12], assuming a one-pole filter behaviour, whose cutoff frequency is estimated from two measurements performed in the acoustic range. Residual errors within ± 50 μV/V are found after corrections in all the considered range.

Information and quantification on phase residual error is generally not given.

Starting from the research activities previously carried out on the characterization and compensation of DMM, this paper proposes a whole characterization of the DCV mode of the 3458A digitizer from a few hertzs up to 100 kHz, considering all the DMM input ranges. The complete frequency characterization of two DMMs allows their use in all combinations of the input configuration. Moreover, each one of them can be replaced by another independently characterised DMM, without need of carrying out again the two instruments characterisation (as done in [7]).

Two different approaches for the identification of the complex filter transfer function (FTF) are proposed and implemented. The first approach considers the input stage of the DMM as a black box; starting from the gain and phase measurements in a frequency range up to hundreds of kilohertz, the FTF structure (number of poles and zeros) in the frequency domain is defined and, through an optimization procedure, the FTF parameters, which best fit the measurements, are sought. Two measurement setups are proposed and implemented to measure the frequency behavior of the DMM. The first system involves two synchronized DMMs: the one under characterization, which operates in DCV sampling mode and the reference one, which works in dc coupled direct sampling (DSDC) mode. By this setup the complex frequency behavior of the DMM when set to DCV mode can be determined. The other measurement setup involves the DMM under test and a high precision calibrator (HPC). By this setup, the frequency behavior of the gain only of the DMM when is set both in DCV and DSDC modes can be determined. In addition, information on the trigger delay can be obtained.

The second approach, which is more physical, identifies the parameters of the electrical circuit of the DMM input stage. By information on the circuit topology given in [10]–[13] and by input impedance measurements, the electrical parameters that best fit the computed impedance frequency behavior to the complex impedance measurements can be set.

Results obtained by the proposed methods are presented, discussed and validated by application to a test case. Comparison is also performed with data obtained by previously proposed methods, extending their application to several tens of kilohertz as well as to the evaluation of the phase behavior for all digitizer ranges.

TABLE I
INPUT IMPEDANCE AND FREQUENCY BANDWIDTH FOR THE DCV MODE

Range	Input impedance	Typical Bandwidth
100 mV	>10 GΩ	80 kHz
1 V	> 10 GΩ	150 kHz
10 V	> 10 GΩ	150 kHz
100 V	10 MΩ	30 kHz
1000 V	10 MΩ	30 kHz

II. METROLOGICAL PERFORMANCES OF THE AGILENT 3458A DIGITIZER

Multimeter Agilent 3458A makes available three different digitizing modes: DCV, DSDC, and subsampling (SSDC). The acquisition chain of the DCV mode involves a signal conditioning stage and an integrating analog-to-digital (A/D) converter with a variable integration time from 500 ns to 1 s and a resolution of 100 ns. The DSDC and SSDC mode makes use of a 12-MHz signal conditioning stage, a track-and-hold circuit and an integrating A/D converter with a 2 ns fixed integration time. In the DSDC the signal is acquired in real time with a maximum sampling frequency of 50 kHz. The sequential or subsampling mode is able to acquire periodic waveforms through the equivalent time algorithm with a maximum equivalent digitizing rate of 100 MHz.

The increase of the aperture time for DCV allows to lower the noise and to increase the equivalent number of bits, with a consequently decreased bandwidth [4]. Thanks to this approach DCV is also the most accurate mode to digitize signals with a limited bandwidth.

Although the DCV mode shows better accuracy performances, it introduces systematic errors in the phase and magnitude of the digitized ac signals. This is due to the different cutoff frequencies at different ranges, as summarized in Table I.

III. SETUP FOR MV AND HV SENSOR CHARACTERIZATION

The need to calibrate electronic voltage sensors, whose output goes from tens of millivolt to tens of volt, in a frequency range up to tens of kilohertz makes the conventional 50-Hz

calibration setups, simply based on the use of a reference voltage transformer (VT) and an analog bridge, unusable. In fact, since the reference and the transducer under test can have different building technologies, their output signals can have considerably different amplitudes. Two synchronized devices such as the Agilent 3458A, offer attractive performances to be effectively used for the measurements of the transducer ratio and phase errors. The selectable ranges from 100 mV to 1000 V can avoid the insertion of other attenuators/amplifiers, otherwise necessary if an acquisition system with fixed input range is used. The high input impedance given by the DCV mode, associated with the selectable aperture time and the higher bit resolution constitute a precious feature for the accurate characterization of sensors. On the contrary, the systematic errors introduced by the input signal conditioning stage of the digitizer can make this approach unusable. Assuming that, for example, the calibration of a voltage divider, with a scale factor of 10000 and a rated voltage of 20 kV, is performed by comparison with a reference VT, with a scale factor of 500 and a rated voltage of 20 kV, then the ranges of the two DMMs will be 10 and 100 V, for the divider and the VT, respectively. In this scenario, assuming, as a first approach, first order filters and rated cutoff frequencies (see Table I), a systematic error of about 1.3 mrad at 50 Hz is introduced in the phase error estimation [14], [15], while at 2.5 kHz the systematic errors become 0.33% and 67 mrad for the ratio error and the phase displacement, respectively. According to the accuracy requirements for the harmonic measurements defined in [1], these errors are unacceptable for a calibration system.

IV. Digitizer Input Frequency Characterization

The frequency behavior of the DMM input filter has been characterized by using two different approaches. The first one, named DCV–DSDC setup, involves two DMMs: that under test is set in DCV mode and the reference one in DSDC mode. The second approach involves a combination of the input impedance measurement in a wide frequency range up to tens of megahertz and a circuit model. Moreover, a second measurement setup for the wideband investigation of the DMM behavior is considered, which involves a voltage calibrator and the DMM under test. By this setup, the frequency behavior of the gain and the trigger phase delay when the DMM is set both in DCV and DSDC modes and the trigger is set in zero-level mode are measured.

A. DCV–DSDC Setup

The DCV–DSDC setup is made of a couple of Agilent 3458A multimeters, externally triggered by a TTL signal given by a Fluke 397. A voltage calibrator Fluke 5500 applies the same signal to the input of the two multimeters as shown in Fig. 1. The first DMM, which is the device under test, operates in DCV sampling mode, while the second DMM, which works as a reference, operates in DSDC mode. The DCV function provides the best accuracy, but the bandwidth is limited (Table I). The acquired signals are processed by the acquisition and analysis software developed in Python. The magnitude of the multimeter transfer function, for each

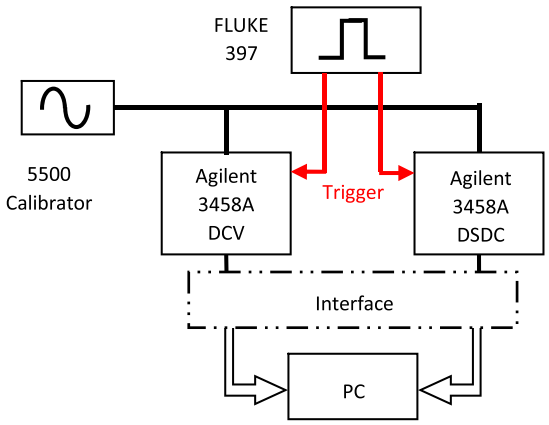

Fig. 1. Measurement setup exploiting DCV and DSDC operating modes.

frequency, is given by the ratio of the DSDC amplitude indication to the DCV one, whereas the phase is obtained as difference between the DCV and DSDC measured phases. The measured values of the multimeter transfer function are the input to the next step, where the analytical function which best approximates the measured data is identified.

The main drawbacks of using a multimeter in DSDC mode are the reduction in the accuracy and the lower maximum sampling frequency, which is limited to 50 kHz [16].

To overcome this limit, exploiting the aliasing phenomenon, a sequential subsampling technique is used. This result is achieved using an appropriate choice of signal (f) and sampling (f_s) frequencies according to

$$\begin{cases} f = \frac{n}{k} \cdot f_S \\ x = \frac{T_S}{k} \\ n = h \cdot k \pm 1 \end{cases} \tag{1}$$

where n is the number of periods used for the modified subsampling technique, k is the number of points per equivalent period, and h is an integer number. Considering the available hardware in this paper, the characterization frequency range has been extended to 100 kHz.

The uncertainty associated with the gain and phase of the digitiser configured in the DCV mode is evaluated by considering the uncertainty component due to the repeatability of the measured values and the contribution due to the reference digitiser working in DSDC. For the 10 V range, the repeatability component, expressed as standard uncertainty, is 100 μV/V (100 μrad) at 10 kHz. The type B uncertainty associated with the amplitude frequency correction, due to the DMM in the DSDC mode, is 100 μV/V. The overall uncertainty is 141 μV/V at 10 kHz. For the phase, the type B uncertainty is due to the rated difference between the trigger latency of the two DMMs involved in the setup, which is 1.6 mrad at 10 kHz (to be compared with a DCV filter error of 90 mrad).

B. Input Impedance Measurement

As described in [9], the input stage impedance of the DMM depends on the selected range. For the 1–10 V

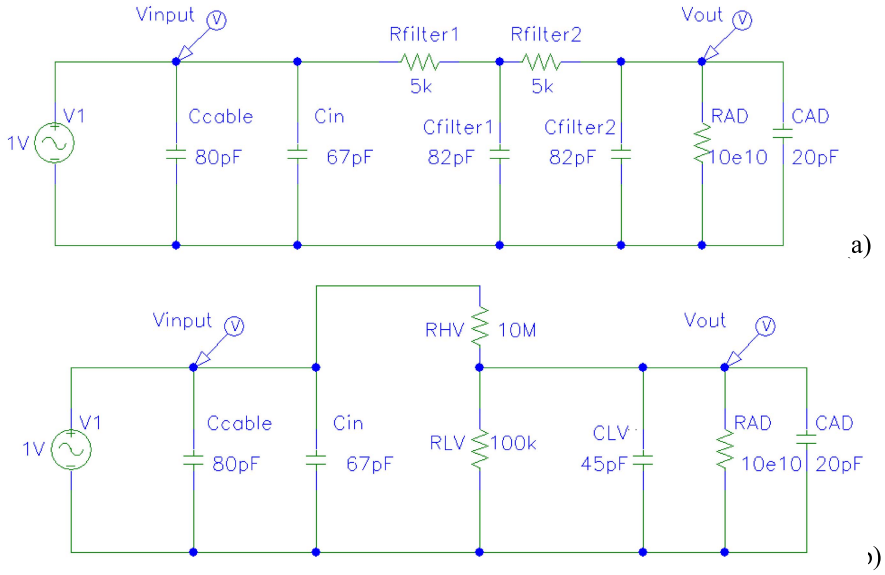

Fig. 2. Input impedance model related to the (a) 1–10 V and (b) 100–1000 V ranges of Agilent 3458A.

and 100–1000 V ranges, the equivalent input circuit is shown in Fig. 2(a) and (b), respectively. The first range is constituted by three sections: an input DMM capacitance, the low-pass filter made of a chain of two *RC* filters and a parallel *RC* bipole representing the A/D input impedance section. For the 100 and 1000 V ranges a resistive divider (RD), which attenuates 100 times the input voltage is connected before the A/D conversion and substitutes the *RC* filter; a capacitance simulating the stray parameter is added in parallel to the output divider.

The 100 mV range has the same impedance of the 1–10 V ranges but a signal amplifier, which gives the overshoot on the gain (Fig. 3), is added before the A/D conversion. As a consequence, the frequency behavior of this amplifier cannot be estimated by the input impedance measurement.

For both configurations, the capacitance C_{cable} of 80 pF simulates the 0.8 m cable connection between the impedance analyzer (IA) and the DMM.

The complex impedance measurements (magnitude and phase) have been performed by employing the following equipment: 1) Keysight 4329 IA 40 Hz–110 MHz; 2) Agilent 3458A multimeter; 3) coaxial cable connecting the IA and the DMM (0.8 m long); and 4) a PC, running a Python measurement software, which controls the execution of the tests.

The impedance circuit model has been developed in the PSPICE tool. The cable connection capacitance has been estimated by measuring the complex impedance when it was disconnected from the DMM. Then, in order to find the right values of the circuit parameters (C_{AD} and C_{in}) a deterministic first-order optimization procedure, in MATLAB environment, has been used. As a first attempt, the measured value of the connection cable capacitance, the rated values for the low-pass filter and the RD given in [9] and [11] as well as the rated resistance of the A/D, given by the DMM manual, have been used. The values of C_{AD} and C_{in} that best matched the measured impedance and input frequency response have been chosen and are, respectively, 20 and 67 pF. The equivalent digitizer input capacitance is found equal to 251 pF for the circuit of Fig. 2(a), which is well within the range of values (from 245 to 263 pF) measured in [13] on different HP digital multimeters.

Considering the deviation between measured and computed impedance, the relative standard uncertainty associated with capitance C_{AD} is conservatively evaluated as 10% for the 10 V range and 1% for the 100 V range. Uncertainties associated with the other rated parameters are conservatively estimated. In detail: 1% for the 5 kΩ resistance and 2% for the 82 pF capacitance are assumed for the 10 V range, 100 $\mu\Omega/\Omega$ is associated with both the 10 MΩ and 100 kΩ divider resistances. Such input uncertainties, propagated through the complex gain analytical expressions of the 10 and 100 V ranges, respectively, provide a standard uncertainty, at 10 kHz, of the gain magnitude (phase) of 120 μV/V (1.3 mrad) and 740 μV/V (2.8 mrad). Such uncertainties are, respectively, 100 and 50 times lower than the evaluated corrections.

C. HPC Setup

The second setup for the measurement of the DMM frequency behavior is constituted by a multimeter Agilent 3458A and a reference calibrator Fluke 5730A, equipped with a voltage amplifier Fluke 5725A. The DMM is characterized both in DCV as well as in DSDC mode, using its internal timebase and trigger. The characterized DMM is a different Agilent multimeter with respect to the one used in the first setup.

The multimeter has been characterized for all the five input voltage ranges, that is from 100 mV to 1 kV. Due to the frequency-amplitude limitations of the utilized hardware, in some ranges the multimeter has been characterized up to 500 kHz (100 mV, 1 V, 10 V), in some other up to 250 kHz (100 V) and 5 kHz (1000 V). The steps of the measurement procedure are as follows:

1) choose the sampling mode;
2) choose the input voltage range;
3) choose signal amplitude;
4) choose signal frequency;
5) choose the sampling frequency;
6) generate the signal;
7) measure the multimeter gain and the waveform phase;
8) repeat Step 7 for ten times;
9) repeat from Step 4 for N_f times;
10) repeat from Step 2 for the remaining input voltage range;
11) repeat from Step 1 for the other sampling mode.

where the sampling modes are DCV and DSDC, the input voltage ranges are 100 mV, 1 V, 10 V, 100 V, 1 kV, N_f is the number of frequencies involved in the procedure. As to the sampling frequency, the same subsampling technique shown in Section IV-A has been used; a sampling frequency equal to 100 times each signal frequency has been used. For each acquisition, 10 000 points have been analyzed and magnitude and phase have been evaluated by using frequency domain interpolation [2].

The reference value for magnitude measurement is the voltage set on the calibrator. As regards the phase measurement, the internal trigger has been used: the first sample is acquired when a trigger event is detected. Thus, setting the trigger with level equal to zero, positive slope and dc coupling, with an ideal triggering circuit the acquired signal should start with zero phase. However, as stated in [4], a contribution of the trigger latency to the measured phase should be considered. Moreover, in DCV sampling mode, the contribution of the aperture time to the measured phase should also be taken into account. As a value of aperture time for DCV sampling mode, 500 ns has been used.

It is worthwhile noting, moreover, that with this second measurement setup the phase response of the input stage of the multimeter cannot be characterized, but the phase measurements refer to the trigger delay. In fact, since the trigger receives the signal from the signal conditioning stage of the multimeter, the acquisition starts on the zero crossing of the filtered signal, so already delayed in phase.

V. Results and Discussion

A. DCV–DSDC Setup

The complex data obtained by the DCV-DSDC measurement setup for the 100 mV range characterization are shown in Fig. 3. Fig. 3(a) and (b) provides a comparison between the magnitude and phase gain behavior measured and computed by considering the one pole (120 kHz)—one zero (82 kHz) transfer function suggested in [9]. For what concerns the magnitude gain, the transfer function provides compatible results up to tens of kilohertz, but the two behaviors strongly diverge over 50 kHz. The behavior of the two phases is completely different: function of [9] provides a positive increasing phase against the measurement behavior, which shows a negative decreasing phase. This confirms that, for the 100 mV range, the instrument cannot be simply represented as a zero-pole first-order filter. Indeed, for the scales at 1 V, 10 V, 100 V and 1 kV the Bode diagrams of both the errors show a slope compatible with a single pole transfer function, but the two characteristics, separately analyzed, correspond to a filter with a pole placed at different frequencies. Furthermore, the behavior of the 100 mV range is different from the others, presenting an amplitude that increases with the frequency while the phase decreases. This mismatch between the amplitude and the phase angle makes the single pole transfer function representation of the DMM behavior unrealistic, confirming that its transfer function must be more complex.

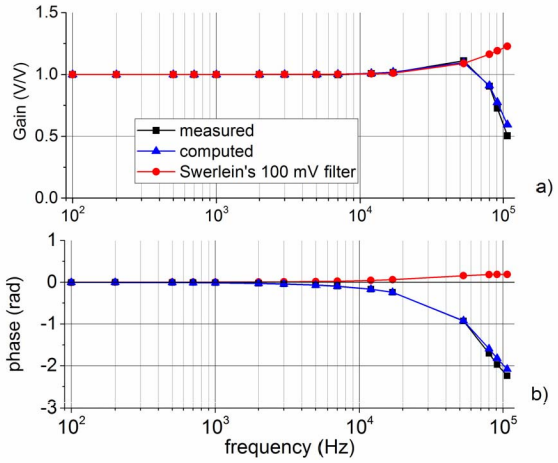

Fig. 3. Comparison between the measured frequency behavior of the 100 mV DMM filter (a) gain and (b) phase, the simulated ones by considering a zero-pole filter (proposed by Swerlein [9]) and by considering a transfer function with one zero and two poles.

For this reason, the frequency behavior of the DMM has been approximated with a transfer function composed by two poles and one zero. A multiobjective optimization problem has been solved to well approximate at the same time the magnitude and the phase characteristics, identifying an optimal combination of poles and zero frequencies to fit each range under test. In some ranges, even with this transfer function, a relevant mismatch is observed between the phase and the magnitude characteristics.

In this cases, a tradeoff between a good representation of the phase and the magnitude is necessary, since several solutions have been identified in the Pareto front. Anyway, a considerable bandwidth extension is achieved through this correction. A transfer function composed by two poles and one zero has been used to approximate all the ranges and it is shown in

$$\frac{V_{out}}{V_{in}} = \frac{1+\frac{s}{\omega_z}}{\left(1+\frac{s}{\omega_{p1}}\right)\left(1+\frac{s}{\omega_{p2}}\right)} \tag{2}$$

where $\omega_z = 2\pi f_z$, $\omega_{p1} = 2\pi f_{p1}$ and $\omega_{p2} = 2\pi f_{p2}$

Only for 100 mV range two complex conjugate poles are assumed, while for the other ranges two real poles are assumed. The expression of the transfer function used for 100 mV range is shown in

$$\frac{V_{\text{out}}}{V_{\text{in}}} = \frac{1+\frac{s}{\omega_z}}{\frac{s^2}{\omega_p^2}+2\xi\frac{s}{\omega_p}+1} \tag{3}$$

where ξ is the damping factor.

TABLE II

ZERO (f_z) AND POLES (f_p) FREQUENCIES OBTAINED FROM THE OPTIMIZATION.

	100 mV		1 V	10 V	100 V	1 kV
f_z (kHz)	405754	f_z (kHz)	259	382	142	56,0
f_p (kHz)	79,2	f_{p1} (kHz)	164	125	52,7	29,5
damping	0,540	f_{p2} (kHz)	241	6407	52,8	873

TABLE III

DEVIATION OF 1 POLE AND COMPLEX FIT FUNCTION FROM MEASURED VALUES FOR 1 V RANGE

frequency (kHz)	1 pole f_{3dB}=115 kHz Ratio	Phase (mrad)	1 zero -2 poles Ratio	Phase (mrad)
17	0.3%	8	0.26%	3.7
50	3%	17	1.6%	4.5
119	16%	47	2.1%	0.1

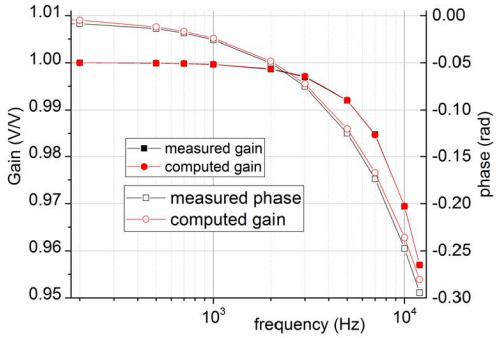

Fig. 4. Comparison between measurement and computation of the 100 V range filter frequency behavior. The computation is performed by a zero two poles function.

As it can be seen from Table II, the range 100 mV is well described simply by a couple of complex conjugate poles, since the zero in the optimal solution is considerably far from the frequencies of interest and so it can be disregarded.

The comparison between measurement results and the ones computed by considering the [9] transfer function provides a deviation of 0.21% for the magnitude and -0.21 rad for the phase. The deviation falls down to -0.14% for the magnitude and 2.2 mrad for the phase when a transfer function with one zero and two complex conjugate poles are considered.

For the range 1 V the second pole is quite close to the zero, so the transfer function is very similar to a single pole, even if not at the rated frequency (100 kHz). For the ranges 10 V, 100 V, and 1 kV the added zero and pole are at higher frequencies, so the correction is more significant. For the 100 V range a comparison between the measured and computed gain and phase is shown in Fig. 4.

For the 1 V range, a comparison between the one-pole fit function, proposed in [9], and the transfer function summarized in Table II is provided in Table III. The best cutoff frequency for the one-pole fit function has been found at 115 kHz. Such frequency provides a deviation from measured data within 70 μV/V and 8 mrad within 5 kHz.

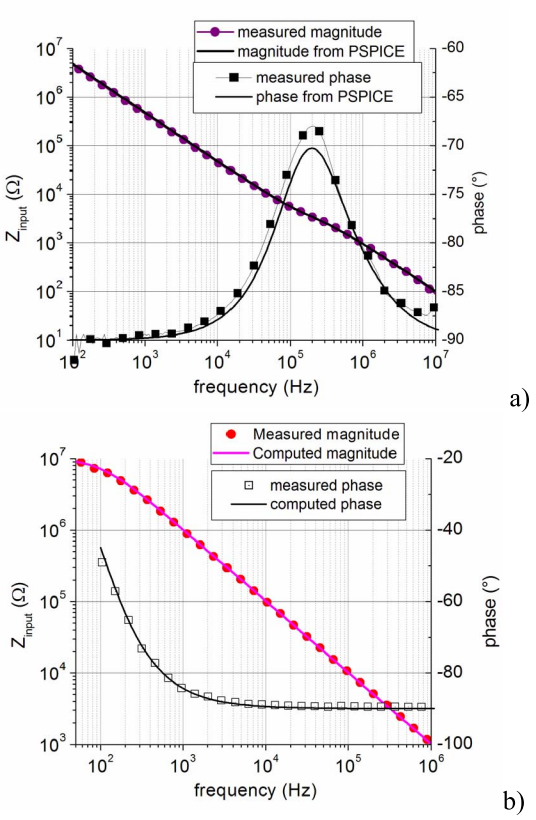

Fig. 5. Magnitude and phase of the impedance frequency behavior for (a) 1 and (b) 100 V.

Table III shows approximately the same performance of the two fit functions in the audio frequency band (17 kHz); for higher frequencies, the simple one-pole function shows higher deviations.

B. Impedance Measurement Results

The frequency filter behavior estimated through the impedance measurement has been applied to the 1 and 100 V ranges. A comparison between measured and simulated impedance frequency behavior is shown in Fig. 5(a) and (b) for 1 V and 100 V, respectively. The complex impedance has been measured, for both the range configurations up to 110 MHz. For the 1 V range the input impedance has a capacitive behavior up to some kilohertz, while, for higher frequencies, the effect of the *RC* chain filter is particularly evident in the phase behavior, which has a Gaussian-like behavior centered around 200 kHz with a maximum of $-67°$. On the contrary, the 100 and 1000 V ranges have a resistive behavior at low frequency and a capacitive behavior from about 100 Hz. Once the circuit parameters are identified, the ratio of the input voltage of the A/D converter stage to the applied voltage (V_{out} and V_{in}, respectively, in Fig. 2), which is the filter gain, can be computed in magnitude and phase. A comparison between measured complex filter gain and computed ones obtained by the identification algorithm with a single pole and with a more complex (one zero, two poles) fit function is shown in Fig. 6(a). From Fig. 6(b), it can be seen that the deviation between PSPICE model and the

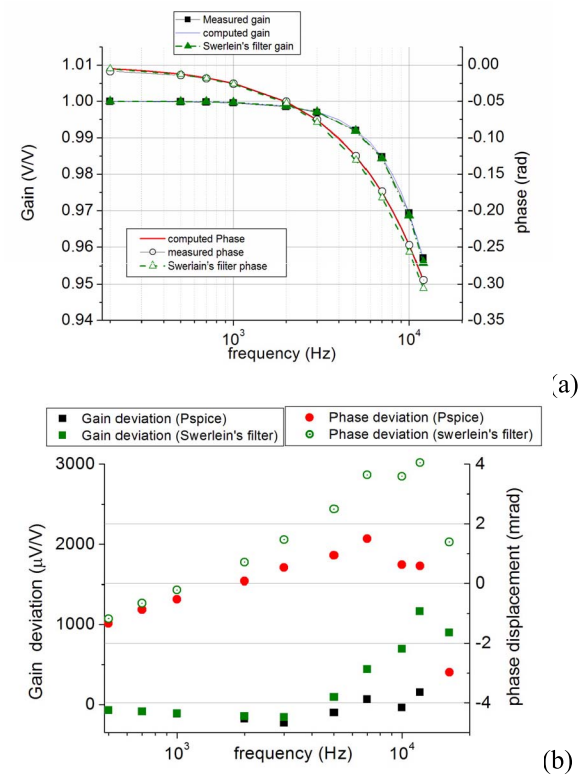

Fig. 6. Gain and phase obtained by the PSPICE model and by one-pole fit function for the 100 V range compared with the measurements given by the (a) DCV–DSDC setup and (b) their deviation.

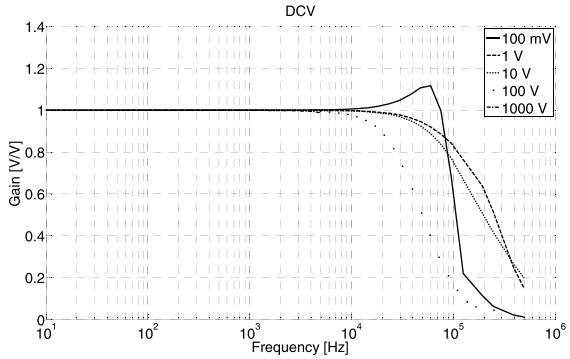

Fig. 7. Gain of the multimeter, in DCV sampling mode, for the different input voltage ranges.

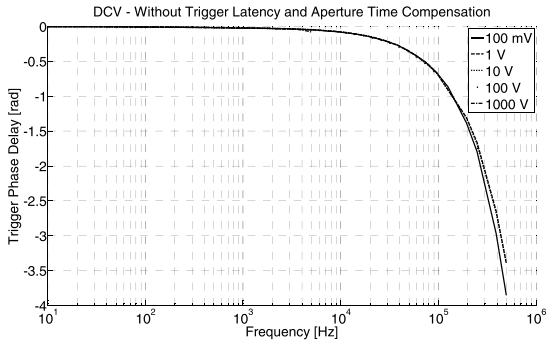

Fig. 8. Trigger phase delay, in DCV sampling mode, for the different input voltage ranges.

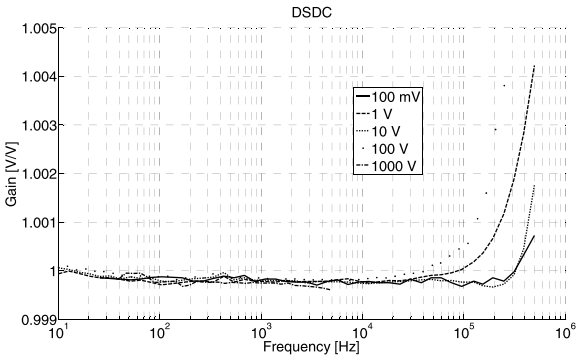

Fig. 9. Gain of the multimeter, in DSDC sampling mode, for the different input voltage ranges.

one-zero, two poles function, for the gain, is within ± 200 μV/V and ± 2 mrad for the phase, for the 100 V range, up to 10 kHz. Higher deviations are found for the one pole ($f_{-3\mathrm{dB}} = 39$ kHz) fit function.

C. High Precision Calibrator and DMM Setup

The data obtained with the calibrator and multimeter setup characterization are shown in Figs. 7–10. Figs. 7 and 8 show, respectively, the gain and the trigger phase delay, in DCV sampling mode, for the five input voltage ranges, whereas Figs. 9 and 10 refer to the DSDC sampling mode.

The trigger phase behavior in Fig. 8 includes the contributions of nominal trigger latency and aperture time; the phase shown in Fig. 10 includes only the contribution of the nominal trigger latency.

Even if these contributions are compensated, the two phase responses are not constant with frequency. This push to consider that the trigger circuit has a frequency dependent behavior. Moreover, even if the two phase responses are compensated, they remain different. Probably, this is due to a different trigger behavior in the two sampling modes. Table IV shows the standard uncertainties, for each range, of the measured magnitude and phase, up to 10 kHz (5 kHz for 1000 V range), using real-time sampling. As regards the gain, the uncertainties for DCV and DSDC are practically the same: this is due to the fact that the B-type uncertainty, which depends on the used calibrator and is the same for both DCV as well as DSDC, is much higher than A-type uncertainty, that is two orders of magnitude for DCV and one order of magnitude for DSDC.

As another proof of the validity of the presented method, the magnitude measured with this setup has been compared with the magnitude measured with the first setup and the frequency response of the magnitude of the identified filter. These three curves, referring to 1 V range, are shown in Fig. 11. As it can be seen, the three curves are very similar and the maximum deviation among them is lower than 100 μV/V at 7 kHz. This is a more valuable result, taking into account that two different DMMs have been considered and two different measurement techniques have been used for their characterization. Fig. 11 also provides the frequency behavior of the transfer function

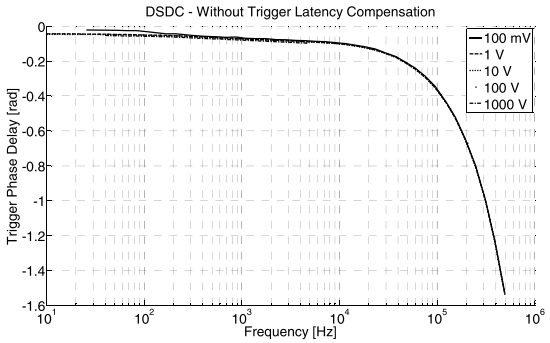

Fig. 10. Trigger phase delay, in DSDC sampling mode, for the different input voltage ranges.

TABLE IV

STANDARD UNCERTAINTIES FOR GAIN AND PHASE, FOR ALL THE INPUT VOLTAGE RANGES

	Gain [μV/V]		Trigger Phase Delay [mrad/rad]	
range	DCV	DSDC	DCV	DSDC
100 mV	71	75	5.8	380
1 V	22	23	4.3	2.8
10 V	20	21	2.7	1.8
100 V	20	21	4.0	2.0
1000 V	53	53	3.1	1.6

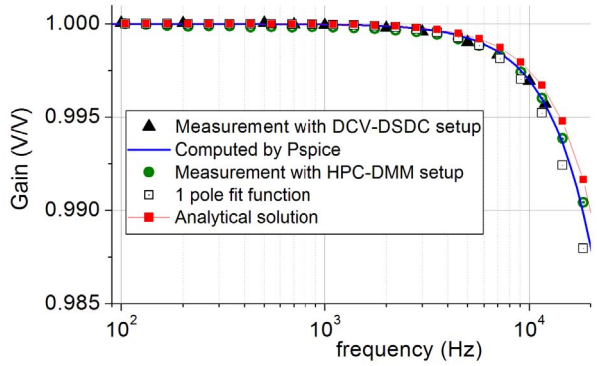

Fig. 11. Frequency behavior of the input filter when 1 V is selected: comparison between the gains measured by the DCV–DSDC and HPC + DMM setup with the ones computed by the PSPICE impedance model, by the one pole fit function and by the analytical solution of the RC filter.

which analytically describes the two-stage *RC* filter that is also proposed in [11]. The rated electrical parameters $R = 5\,\text{k}\Omega$ and $C = 82$ pF are considered. It can be seen that this approach is not as accurate as the other proposed approach. This can be explained by the fact that the two *RC* stage filter is actually connected to a capacitive load which was not considered in [11].

D. Divider Frequency Characterization

As a test of the performances of the DCV–DSDC compensation method, the measurement of the frequency response of an adjusting *RC* network, designed to correct the frequency behavior of a 30-kV divider, has been carried out.

The rated frequency behavior of this network is like that of a *RC* divider not exactly compensated, the phase error reaches

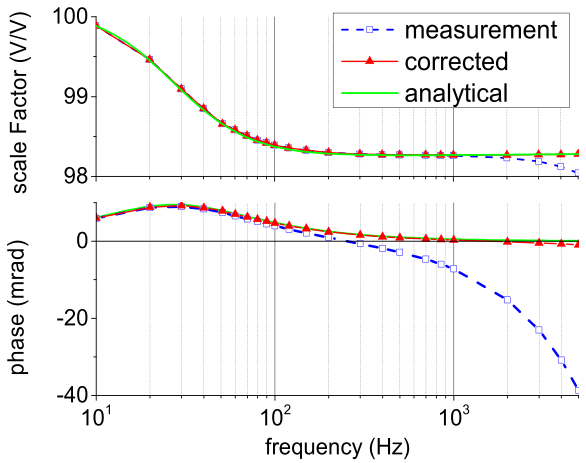

Fig. 12. Comparison between analytical, measured, and corrected divider scale factor and phase.

a peak around 30 Hz and ideally goes asymptoticcally to zero at the increase of the frequency.

Measurements were carried out by applying a sinusoidal voltage (100 V) at increasing frequencies from 10 Hz to 40 kHz by a Fluke 5500 calibrator and by measuring the applied and the divider output voltage with two Agilent 3458A DMMs, respectively, both operating in DCV mode. The measured divider scale factor (ratio of the divider input to ouput voltage) and phase error values were measured with and without corrections as evaluated by the DCV–DSDC setup.

Fig. 12 highlights the strong deviation, at high frequency, between the measured scale factor and phase from the computed ones (analytical), computed from the divider circuit model, using the measured values of the circuit parameters. The application of the corrections (corrected data) considerably reduces the discrepancy between the measured and computed data. This phase error has been evaluated as 12 and 54 mrad at 1 and 10 kHz, respectively. At the same frequencies, the residual deviation between computed and corrected waveforms is within 0.2 and 1.8 mrad, proving the validity of the proposed method.

VI. CONCLUSION

Thanks to the metrological performances and the available input ranges (from 100 mV to 1 kV), the use of a synchronized couple of digitizers Agilent 3458A working in DCV mode can allow the accurate measurement of the ratio error and phase errors of voltage and current sensors by comparison with reference ones. The factor limiting their use is the systematic errors introduced by the DMM input filter, which has then to be corrected.

The methods proposed in the paper (the black-box approach with DCV–DSDC and the input impedance measurement approach) allow the improvement of the DMM performances through identification of a complex filter reproducing its frequency behavior both in magnitude and in phase, for all the input voltage ranges, allowing the implementation of suitable corrections.

The results obtained in the characterization of the same DMM by the two approaches are found equivalent considering the associated uncertainties. However, the DMM 100 mV range can be characterized only by the black-box approach with DCV–DSDC measurement setup that is then the most complete one. The filters so identified show deviations from the measured frequency responses of 200 μV/V for the magnitude and 2 mrad for the phase up to 10 kHz. As a final test of the reliability of the black-box compensation technique, the frequency response of a well characterized 100 V/1 V voltage divider has been measured with two DMMs, with and without compensation. At 1 kHz, the difference between the known and the measured phase responses reduces from 12 mrad, without compensation, to 0.2 mrad, with compensation.

Comparison with different approaches based on the use of one-pole and two-pole filter highlights how the presented techniques extend the performance of already proposed methods in a wider frequency range, up to tens of kilohertz.

REFERENCES

[1] *IEC/TR Instrument Transformers—The Use of Instrument Transformers for Power Quality Measurements*, document IEC/TR61869-103, 2012.

[2] G. Crotti, D. Gallo, D. Giordano, C. Landi, M. Luiso, and M. Modarres, "Frequency calibration of MV voltage transformer under actual waveforms," in *Proc. Conf. Precis. Electromagn. Meas. (CPEM)*, Ottawa, ON, Canada, Jul. 2016, pp. 1–2.

[3] J. De La Ree, V. Centeno, J. S. Thorp, and A. G. Phadke, "Synchronized phasor measurement applications in power systems," *IEEE Trans. Smart Grid*, vol. 1, no. 1, pp. 20–27, Jun. 2010.

[4] Agilent Technologies. (2012). *3458A Multimeter User's Guide Edition 5, U.S.A*. [Online]. Available: http://cp.literature.agilent.com/litweb/pdf/03458-90014.pdf.Ronald

[5] W. G. K. Ihlenfeld, E. Mohns, H. Bachmair, G. Ramm, and H. Moser, "Evaluation of the synchronous generation and sampling technique," *IEEE Trans. Instrum. Meas.*, vol. 52, no. 2, pp. 371–374, Apr. 2003.

[6] W. G. Kurten *et al.*, "Characterization of a high-resolution analog-to-digital converter with a Josephson AC voltage source," *IEEE Trans. Instrum. Meas.*, vol. 54, no. 2, pp. 649–652, Apr. 2005.

[7] D. Ilic and J. Butorac, "Use of precise digital voltmeters for phase measurements," *IEEE Trans. Instrum. Meas.*, vol. 50, no. 2, pp. 449–452, Apr. 2001.

[8] T. J. Stewart, "Spectral leakage errors when using an Agilent 3458A to measure phase at mains power frequencies," in *Proc. Conf. Precis. Electromagn. Meas. (CPEM)*, Washington, DC, USA, 2012, pp. 278–279.

[9] L. Swerlein, *A 10ppm Accurate Digital AC Measurement Algorithm*, Hewlett Packard Co, Palo Alto, CA, USA, Aug. 1991.

[10] G. B. Gubler, "Reconstruction of bandlimited signal using samples obtained from integration digital voltmeters," in *Proc. Conf. Precis. Electromagn. Meas. (CPEM)*, Washington, DC, USA, Jun. 2010, pp. 257–258.

[11] P. Espel, A. Poletaeff, and A. Bounouh, "Characterization of analogue-to-digital converters of a commercial digital voltmeter in the 20 Hz to 400 Hz frequency range," *Metrologia*, vol. 46, no. 5, pp. 578–584, Sep. 2009.

[12] R. Lapuh, B. Voljč, and M. Lindič, "Accurate measurement of AC voltage in audio band using Agilent 3458A sampling capability," in *Proc. Conf. Precis. Electromagn. Meas. (CPEM)*, Rio de Janeiro, Brazil, Aug. 2014, pp. 740–741.

[13] I. Lenicek, D. Ilic, and R. Malaric, "Determination of high-resolution digital voltmeter input parameters," *IEEE Trans. Instrum. Meas.*, vol. 57, no. 8, pp. 1685–1688, Aug. 2008.

[14] G. Crotti, D. Giordano, D. Bartalesi, C. Cherbaucich, and P. Mazza, "Set-up of calibration systems for inductive and electronic measurement transformers," in *Proc. IEEE Int. Workshop Appl. Meas. Power Syst. (AMPS)*, Aachen, Germany, Sep. 2013, pp. 24–28.

[15] G. Crotti *et al.*, "Low cost measurement equipment for the accurate calibration of voltage and current transducers," in *Proc. I2MTC*, Montevideo, Uruguay, May 2014, pp. 202–206.

[16] D. Giordano, P. Pescetto, G. Crotti, and M. Luiso, "Improvement of Agilent 3458A performances in wideband complex transfer function measurement," in *Proc. CPEM*, Ottawa, ON, Canada, Jul. 2016, pp. 1–2.

Gabriella Crotti received the Laurea summa cum laude degree in physics from the University of Torino, Turin, Italy, in 1986.

Since 1986, she has been with the Istituto Nazionale di Ricerca Metrologica, Turin, where she is currently a Senior Technologist with the Energy and Environment Group, Metrology for the Quality of Life Division. Her current research interests include the development and characterization of references and measurement techniques in the field of high currents and high voltages and on the traceability of electric and magnetic field measurements at low and intermediate-frequency.

Domenico Giordano received the Ph.D. degree in electrical engineering from the Politecnico di Torino, Turin, Italy, in 2007.

Since 2010, he has been a Researcher with the Electromagnetic Division, Istituto Nazionale di Ricerca Metrologica, Turin. His current research interests include the development and characterization of systems and voltage/current transducers for calibration and power quality measurements on medium voltage grids, the study of ferroresonance phenomena, and the development of generation and measurement systems of electromagnetic fields for calibration and dosimetric purposes.

Mario Luiso (S'07–M'08) was born in Naples, Italy, in 1981. He received the Laurea (summa cum laude) degree in electronic engineering and the Ph.D. degree in electrical energy conversion from the University of Campania "Luigi Vanvitelli" (formerly Second University of Naples), Aversa, Italy, in 2005 and 2007, respectively.

He currently is an Assistant Professor with the Department of Industrial and Information Engineering, University of Campania "Luigi Vanvitelli." His current research interests include the development of innovative methods, sensors and instrumentation for measurement of electrical and, generally, physical quantities.

Dr. Luiso is a member of the IEEE Instrumentation and Measurement Society.

Paolo Pescetto received the B.Sc. and M.Sc. (with full grade and Hons.) degrees from the Politecnico di Torino, Turin, Italy, in 2013 and 2015, respectively, where he is currently pursuing the Ph.D. degree.

In 2015, he was an Erasmus Student at the Norwegian University of Science and Technology, Trondheim, Norway. He has authored or co-authored three journal and three conference papers. His cur-rent research interests include synchronous motor drives, sensorless control, and self-commissioning techniques.

Mr. Pescetto was a recipient of the Best Paper Award in Renewable Energies at the 2015 International Conference on Ecological Vehicles and Renewable Energies and the Best Paper Award at the 2016 International Conference on Electrical Machines.